Applied Ocean Research 152 (2024) 104184

Contents lists available at ScienceDirect

Applied Ocean Research

journal homepage: www.elsevier.com/locate/apor

"Assessment of combined wind and wave energy in European coastal waters using satellite altimetry."

Sonia Ponce de León [a,*], João Horta Bettencourt [b,c], John V. Ringwood [d], Jérôme Benveniste [e]

[a] Centre for Marine Technology and Engineering, Instituto Superior Técnico, Lisbon, Portugal
[b] Geophysical Institute, University of Bergen, Bergen, Norway
[c] Bjerknes Centre for Climate Change Research, Bergen, Norway
[d] Center for Ocean Energy Research, Maynooth University, Ireland
[e] European Space Agency-ESRIN, Frascati, Italy

ARTICLE INFO

Keywords:
Sea state
Climate change initiative
Satellite altimetry
Wave energy resources
Wave power density
Wind energy resource
European shelf

ABSTRACT

In this study, the combined wind and wave energy potential assessment is presented for various locations in European coastal waters. The objective is to investigate the feasibility of satellite altimetry-based assessments of combined wind/wave renewable energy potential on the European shelf. The study is motivated by the potential reduction in energy supply variability by combining wind and wave. The method consists of using a homogenized multi-mission altimeter database available by the European Space Agency Sea State Climate Change Initiative (Sea_State_cci) that comprises 26 years of data, from January 1991 to December 2018, that allows extending the time range and spatial coverage to estimate site wind and wave power densities. An empirical model is used to estimate the wave energy period from the altimeter Ku band significant wave height and radar backscatter coefficient required to compute the wave power density. The results show that wind/wave energy is relatively correlated in the Mediterranean but not in the North Atlantic sites studied. Thus, the Western North Atlantic sites are the most adequate places for wind and wave farms, from the point of view of combined exploitation.

The different characteristics of the studied sites show some correspondence between variability and mean wave power, which is an essential input to a marine renewable energy strategy in any jurisdiction. The level of overall variability decreases with an increase in mean wave power, related to the higher power swell waves are not highly correlated with the local wind.

1. Introduction

Wave energy conversion technology has significant benefits to society in providing an additional (currently untapped) sustainable energy source that can contribute to the renewable energy mix. Oceans are a significant renewable energy resource (Pontes, 1998) that can contribute to the energy transition towards a green economy. With a drive to 100 % renewable energy, it is important that complementarity between individual renewable (including marine) energy resources, so that the most resilient forms of renewable energy, and combinations of renewable sources are developed.

The intermittency and efficiency of the supply from renewable energy sources is a major concern in the shift from a fossil fuel to a renewable energy powered grid. The combination of offshore wind with wave energy can mitigate these concerns by reducing the variability and downtime of the power supply and increasing its efficiency (Astariz and Iglesias, 2016; Fusco et al., 2010; Stoutenburg and Jacobson, 2010). Overall, co-located offshore wind turbines and wave energy converters can significantly increase the competitiveness of marine renewable energy, by achieving reduced energy costs, improved power output variability and security and a consistent and reliable delivery of renewable power (Astariz and Iglesias, 2017; Stoutenburg and Jacobson, 2010).

The west coast of Europe shows high wave energy potential due to the high energy swells generated by the extra-tropical cyclones that regularly cross the North Atlantic (Gallagher et al., 2014; Iglesias and Carballo, 2010; Ponce de León and Bettencourt, 2021; Mota and Pinto, 2014). In the Western Mediterranean, the highest wave energy density is found to the North of the Balearic Islands and diminishing towards the

* Corresponding author.
E-mail address: soniaponcedeleon@tecnico.ulisboa.pt (S. Ponce de León).

https://doi.org/10.1016/j.apor.2024.104184
Received 21 August 2023; Received in revised form 13 August 2024; Accepted 14 August 2024
Available online 19 August 2024

south due to the sheltering effect and changes in the wave direction. There is a large seasonal variation in the energy flux, being 6 times larger in winter than during the summer (Ponce de León et al., 2016).

Wind energy is the leading form of renewable energy in Europe (deCastro et al., 2019). Offshore winds are advantageous when compared to onshore wind farms because of higher wind speeds in the ocean and the availability of larger areas (deCastro et al., 2019), although the level of the resource varies greatly with location in the European coasts (Carvalho et al., 2014, 2017; Kalogeri et al., 2017; Soukissian et al., 2017)

To date, significant effort has gone into the individual mapping of wind and wave renewable energy resources, with less attention focused on their temporal correlation. The temporal correlation of wind and wave energy significantly affects the combined wind and wave energy resource extraction. Low temporal correlation between wind and wave resources leads to less variable power output and to more stable and predictable conditions, reducing the downtime periods (Martini et al., 2018; Stoutenburg et al., 2010).

Most assessments of wind and wave energy rely on numerical models, but the choice of numerical model and parameterizations is a recognized source of variability in wind and wave energy assessments (Ambühl et al., 2014; Brown et al., 2013; Chen and Yu, 2017; Probst and Cárdenas, 2010). This has impacts in the estimation of the time correlation between wind and wave energy as, e.g., a lower significant wave height (H_s) in a situation of high wind speed may result in a lower time correlation than the actual one.

One way of remediating this is to use concurrent measurements of wind speed and wave height and period, allowing the estimation of wind and wave energy from a single source of data, such as remote sensing. For wave energy assessments, the use of remote sensing has been included in a global oceanic wave energy resource dataset (Zheng, 2021). Ponce de León et al. (2023) and Ponce de León et al. (2024), used satellite altimetry data to assess the wave resource in the French Façade.

Space borne radar altimeters, which can measure H_s and surface wind directly and the wave period can be derived from the H_s and the normalised radar cross section σ^0 (see Zhao et al., 2012 and references therein). Their global coverage and relatively long instrumental record makes them an attractive way of estimating wave energy resources (Yaakob et al., 2016; Goddijn-Murphy et al., 2015; Wan et al., 2016), in particular in those areas were high-resolution hindcasts are not available as in South American or the African coastal zones (Guillou et al., 2020). Also, since altimeters provide concurrent measurements of wave height and near surface wind speeds, together with the wave periods estimates, they are a platform of choice to understand the correlations between wind and wave energy potential on specific sites. In particular, the ESA Sea State CCI (SS_cci) (Dodet et al., 2020) provides a homogenized global multi-mission altimeter climatic data record, including missions from 1991 to 2018 present.

The objectives of this study are to investigate the feasibility of satellite altimetry-based assessments of combined wind/wave renewable energy potential on the European shelf. In particular, this study will attempt to understand how the wind and waves are correlated in the North Atlantic and the Mediterranean, which are two areas with different wind and wave characteristics.

The remainder of the paper is structured as follows: Section 2 is devoted to the materials and methods, where the altimetry data set used is described as well as the statistical coefficients used in the study. Section 3 compiles the results, where is presented the validation of the wave period estimates, the wind and wave power correlations and the coefficients of variations estimated at selected sites in Ireland and around the Iberian Peninsula. In Section 4, the main findings are discussed and in Section 5, conclusions are given.

2. Materials and methods

2.1. Wave and wind power

For real seas, the wave power density (energy flux) P_a in Wm^{-1} of wave front can be computed as (Kalogeri et al. (2017)):

$$P_a = \frac{\rho g^2 H_s^2 T_e}{64\pi}, \tag{1}$$

where ρ is the sea water density (1025 kg m^{-3}), g is the acceleration of gravity (9.81 m s^{-2}), H_s is the significant wave height in meters (the mean of the 1/3 highest waves) and T_e is the energy period in seconds, defined by:

$$T_e = \frac{m_{-1}}{m_0}, \tag{2}$$

where m_n is the n-th order moment of the wave spectrum. The energy period T_e can be derived from the zero-crossing period T_z as $T_e = 1.18\ T_z$, for a JONSWAP spectrum with $\gamma = 3.3$ (Cahill and Lewis, 2014).

The wind power density (power per unit area) P_w in Wm^{-2} is calculated by means of the following expression (Kalogeri et al. (2017)):

$$P_w = \frac{1}{2}\rho_a U_w^3, \tag{3}$$

where ρ_a is the air density (1 kg m^{-3}) and U_w is the wind speed (m s^{-1}) at hub height z_H of 80 m.

2.2. The wave period empirical model

Using altimetry data, we have H_s directly from the altimeter, but we need to estimate T_z. The empirical model of Gommenginger et al. (2003) allows estimating the wave period, required for the computation of the wave power density (1), from the Ku-band radar altimeter H_s and radar backscatter coefficient σ^0.

In the empirical model there is a linear relationship between the quantity $X = 0.25(\sigma^0 H_s^2)$ and T_z:

$$T_z = aX + b, \tag{4}$$

where a and b are coefficients to be computed by linear regression between X, computed with the altimeter H_s and σ^0, and T_z, obtained from wave buoys.

A collocation of the altimeter and buoy measurements must be performed to get (X, T_z) pairs. In our collocation procedure we match up satellite and buoy data that coincide in time inside a 20-minutes window around the time of the buoy datum and are less than 100 km apart. Since the altimeter ground track resolution is much higher than 100 km, there are several altimeter data inside the 100 km circle centered on the buoy location. We average these data to compute the collocated altimeter data of H_s and σ^0. With this procedure we obtain a time series of satellite data collocated with buoy data. The average time interval between collocated data varies depending on the position of the buoy and the period of the buoy data. This is because the number of altimeter missions in the database changes with time as the missions are launched and terminated. For the buoy locations of the study the average interval between time series data is between 1 and 3 days.

2.3. The altimetry dataset

We used version 1.1 of the ESA Sea State CCI database of merged and reprocessed altimeter measurements (Abdalla et al., 2021; Dodet et al., 2020; Piollé et al., 2020). The SS-CCI database used spans the years from 1991 to 2018 (27 years) and included the ERS1, ERS2, TOPEX, ENVISAT, GFO, Cryosat-2, Jason-1, Jason-2, Jason-3 and SARAL/Altika altimeter missions. Except for SARAL/Altika (Ka-band), all altimeters are bi-frequency (Ku/C or Ku/S bands), but only the Ku-band

measurements were used for consistency. SS_cci is a continuation of the GlobWave project (Globwave Team, 2013), with three additional altimeters: Jason-3, Cryosat-2, SARAL/Altika. Altimeter Hs cross-calibration of these additional missions was carried out by comparing Hs measurements at cross-over locations between those altimeters and the reference mission JASON-2.

In this work, the denoised Hs data was used. Denoised Hs was obtained by application of the Empirical Mode Decomposition method (Huang et al., 1998; Quilfen and Chapron, 2021). The overall metrics for denoised H_s against in situ data located more than 200 km from shore ranged between −7 cm and 10 cm for bias and between 20 cm and 26 cm for RMSE.

2.4. Coefficients of correlation and variability

To measure the correlation between the wind and wave renewable energy resources, we used the Pearson correlation coefficient τ of the wind and wave power densities time series:

$$\tau(P_a,P_w)=\frac{1}{N}\sum_{i=1}^{N}\frac{\left(P_{a,i}-\underline{P}_a\right)\left(P_{w,i}-\underline{P}_w\right)}{\sigma_{P_a}\sigma_{P_w}}, \tag{5}$$

where N is the length of the time series, $P_{a,i}$ and $P_{w,i}$ are the i^{th} elements of the wave and wind power densities time series, $\underline{P}_a$ and $\underline{P}_w$ are the wave and wind power densities time series averages, and σ_{P_a} and σ_{P_w} are the wave and wind power densities time series standard deviations. The correlation given by (5) varies between $\tau(P_a,P_w)=-1$, which indicates that the resources are inversely correlated, i.e., when one is increasing, the other decreases, and $\tau(P_a,P_w)=1$, which says that the resources are directly correlated, i.e. they increase or decrease simultaneously. If the resources are uncorrelated, then $\tau(P_a,P_w)=0$.

To measure the variability of the wind and wave renewable energy resources, we use the coefficient of variation (COV) and the seasonal variability indicator (SVI) following Ringwood and Brandle (2015).

The COV is the wave or wind density time series standard deviation σ_P normalized by the wave or wind power density time series average $\underline{P}$:

$$COV=\frac{\sigma_P}{\underline{P}}, \tag{6}$$

The SVI is calculated by:

$$SVI=\frac{P_{max}-P_{min}}{\underline{P}}, \tag{7}$$

where P_{max} and P_{min} are the maximum and minimum of the wave or wind power density time series.

3. Results

The correlation between wave and wind energy was assessed in the west coast of Ireland, the north and west coasts of the Iberian Peninsula, and the western Mediterranean (Fig. 1).

3.1. Validation of wave parameters

This section presents the validation of the wave period T_z and the H_s. The method of Gommenginger et al. (2003) was already extensively validated by several authors. Fig. 2a shows the buoy T_z estimated by (4), against H_s calculated from the Cabo Silleiro wave buoy data. The scatter plot indicates the density of data points and shows a strong correlation with H_s for T_z. However, some dispersion can be seen for the higher periods. On the other hand, for the H_s (Fig. 2b), the correlation between the altimeter and the Cabo Silleiro buoy data is high, as can be seen with a correlation coefficient of 0.94, with a negative bias of −0.124 (buoy data are underestimated) and a scatter index of 0.18. During the 27 years studied, the maximum H_s at Cabo Silleiro was about 8 m. Regarding the Hs buoy – satellite correlation for the other buoys (Fig. 2, panels c – h), it deserves to be mentioned the relatively high bias at M6 (0.255 m; Fig. 2d) and the high scatter index of 0.39 at Cabo Begur (Fig. 2h), which also has the lowest correlation coefficient (0.84).

The comparison of the buoy and satellite estimates of the wave period (Fig. 3) show that the method tendentially overestimate the period in the lower range and underestimates the upper range of the wave period (the best fit line slopes are all < 1). The bias in the wave period estimates is zero due to the use of linear least squares in the regression of (4). The root mean square error (rms) between the buoy and satellite wave periods are shown in Table 1. The rms errors are close to 1 s, except for the Villano-Zisargas buoy that has an rms error of 1.88 s.

The correlation coefficients computed using the satellite data are higher than those of the buoy. This is due to the collocation of the altimeter and buoy observations performed that uses 100 km as the maximum distance of the satellite observation from the wave buoy and could be explained by the lack of Irish wave buoy data. As can be seen from Table 1, the highest correlation was obtained in the Mediterranean Sea at Dragonera (0.810 estimated with satellite observations), where the sea state is characterized by wind sea. The lowest correlation was obtained in the North Atlantic at Cabo Silleiro and Villano-Zisargas. At the same time, relatively high values are representative of the Irish locations where the sea state is dominated mostly by the swell.

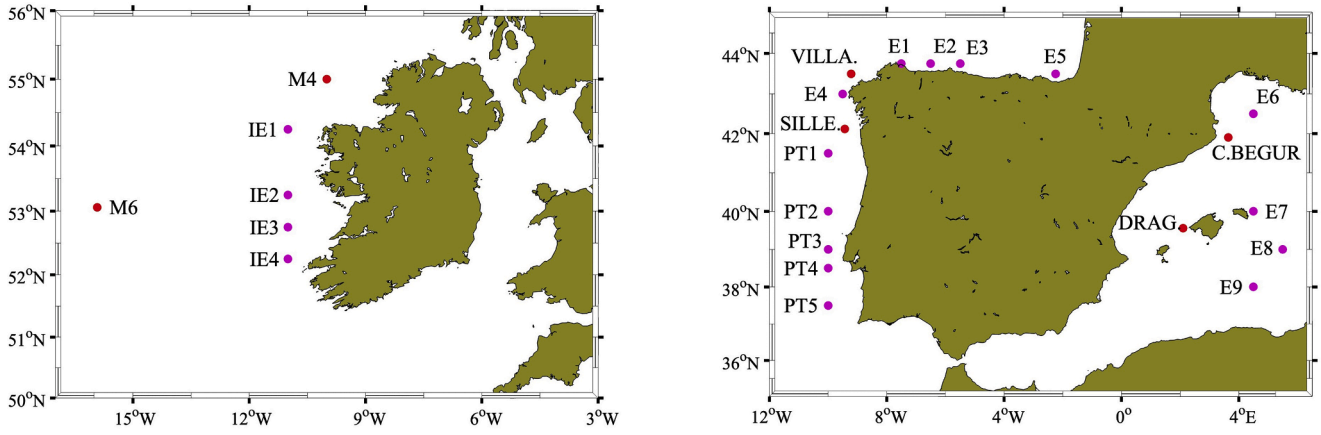

Fig. 1. Buoy (red circles) and wave and wind power assessment locations (magenta circles). (left) West coast of Ireland. (right) Iberian Peninsula and Western Mediterranean. VILLA.: Villano-Zisargas; SILLE.: Cabo Silleiro; G. CAD: Gulf of Cadiz; C. BEGUR: Cabo Begur; TARRAG.: Tarragona; DRAG.: Dragonera.

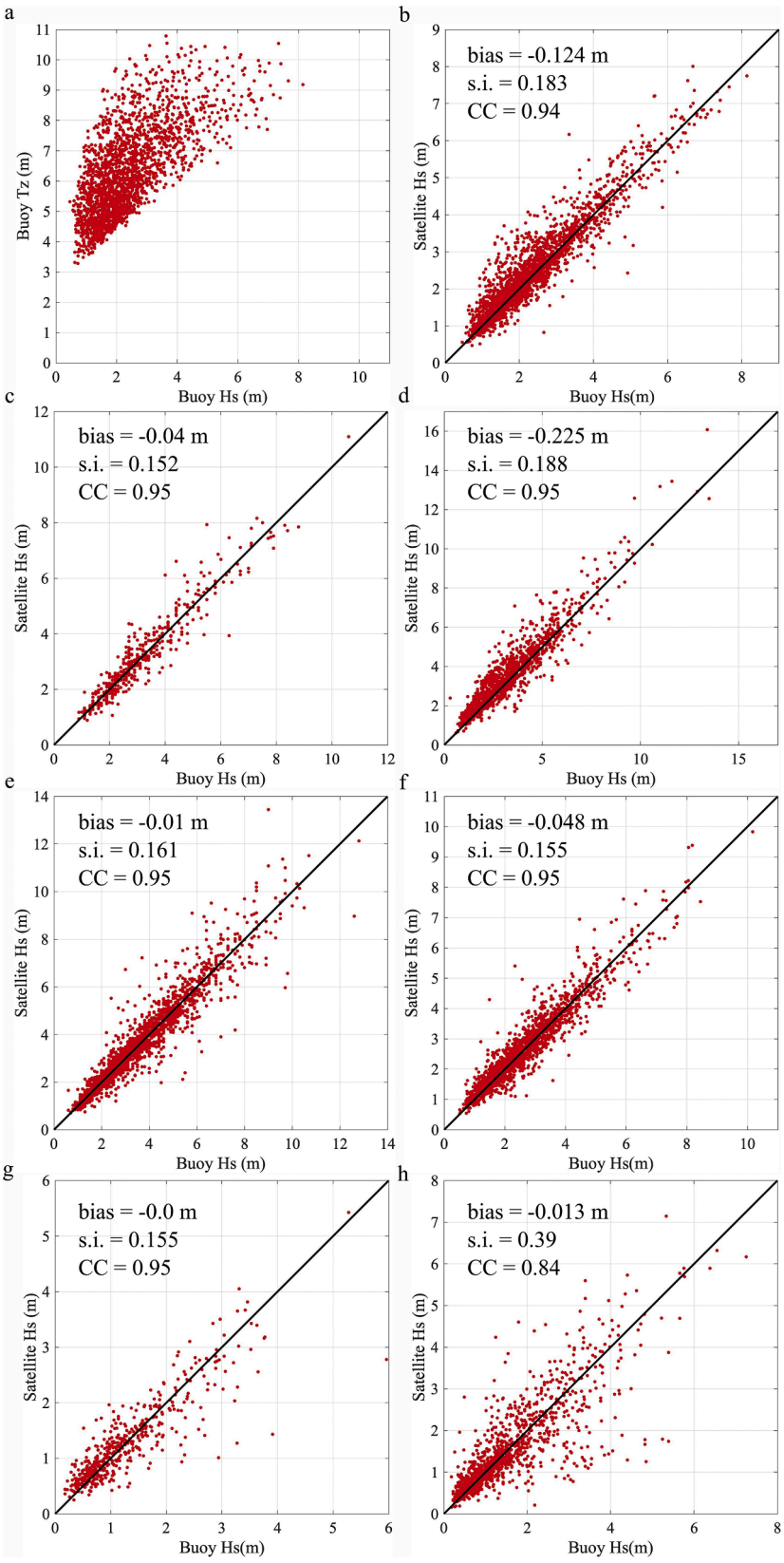

Fig. 2. a) zero-crossing period vs H_s at Silleiro buoy; b) Satellite H_s vs Buoy H_s (45° line in black); c) same as b) for M4 buoy; d) idem for M6 buoy; e) idem for K5 buoy; f) idem for Villano-Zisargas buoy; g) idem for Dragonera buoy; h) idem for Cabo Begur buoy; s.i: scatter index; CC: correlation coefficient.

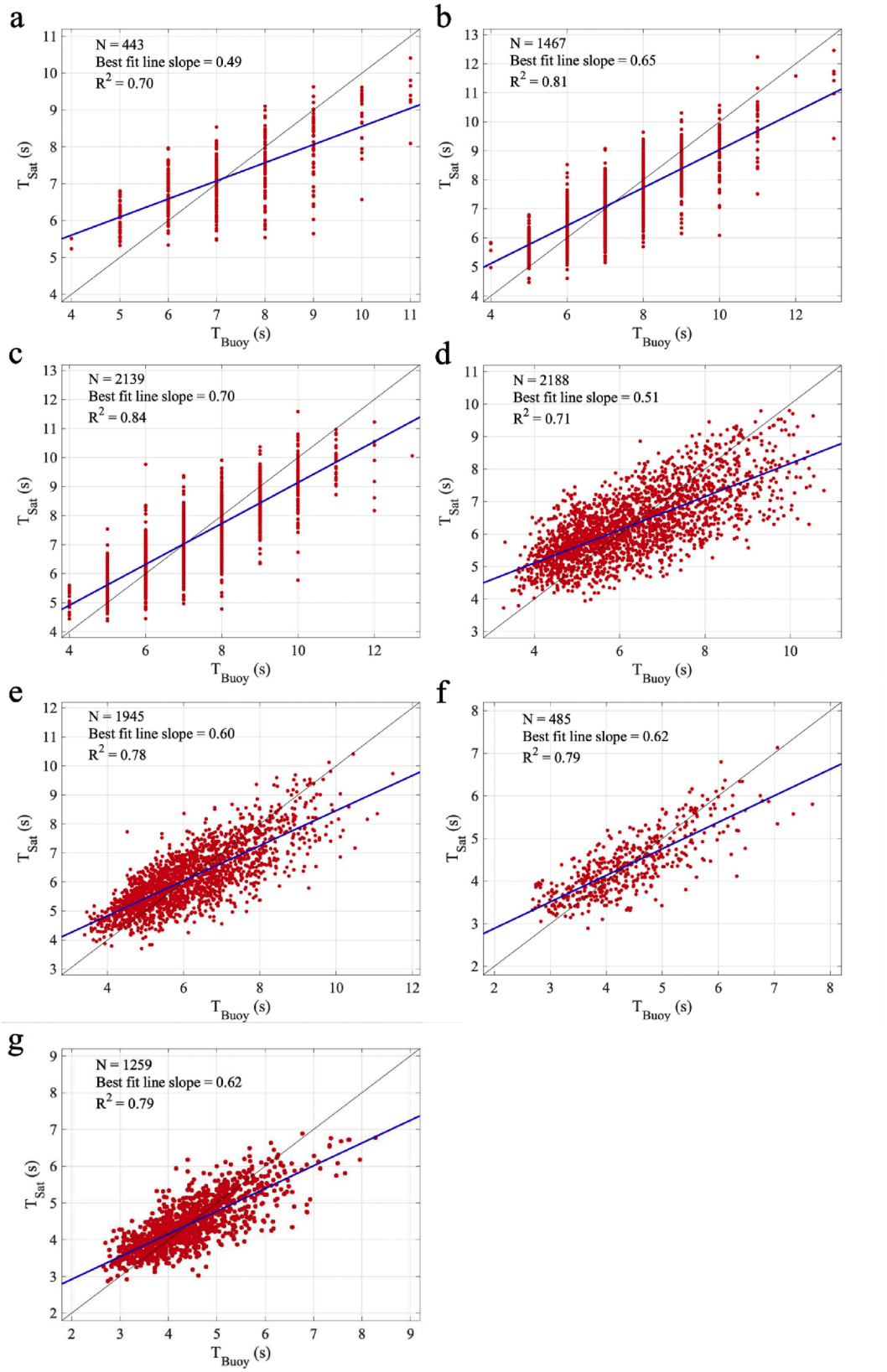

Fig. 3. Buoy and Satellite period scatter plots. a) M4; b) M6; c) K5; d) Cabo Silleiro; e) Villano-Zisargas; f) Dragonera; g) Cabo Begur. For the Irish buoys M4, M6 and K5, the period values were rounded to the nearest integer.

Table 1
Root mean square errors of the energy period estimates and zero-lag correlation coefficients between the wind speed and the Hs estimated from the satellite altimetry data and buoys. Note: τ(Hs,Uw)-Zero-lag correlation coefficient; PAS-Port Authority of Spain; ME-Met Éireann-Ireland's National Meteorological Service, UKMO-UK Met Office.

North Atlantic Buoys	Period (Years)	RMS Te (s)	τ(Hs, Uw) satellite	τ(Hs,Uw) Buoy
M4 (ME)	(2009–2018)	0.98	0.771	0.617
M6 (ME)	(2008–2018)	0.83	0.664	0.705
Cabo Silleiro (PAS)	(1999–2018)	1.02	0.468	0.258
Villano-Zisargas (PAS)	(1999–2018)	1.88	0.501	0.371
K5 (UKMO)	(1999–2018)	0.79	0.728	0.653
Mediterranean Buoys				
Dragonera (PAS)	(2007–2018)	1.18	0.810	0.657

3.2. Wave and wind power resources

Wave and wind energy time series were computed in the four wave power assessment location sets (see Fig. 1). The length of the data period and the number of observations used to compute the energy resource time series is shown in Table 2. The length of the observational datasets spans the years 1991–2018 for all zones, but the average number of observations varies with zone and within zones. The zone with the greatest number of observations is Ireland, while Spain Atlantic has the lowest number of observations, likely due to the fact that these locations are closest to the coast than the others. But many other factors can cause variability in this quantity, since there are several factors affecting the validity of the altimeter observations, such as the occurrence of rain.

Wind power resources show a marked variation between the study sites (Fig. 4a). The highest wind power is registered in the west coast of Ireland, with values between 1000 and 1500 W/m2, which compare to the estimates of Kalogeri et al. (2017) for the same zone. The values for Portugal and Atlantic Spain (PT1–5 and E1–5 in Fig. 4a) also compare well to the results of Kalogeri et al. (2017), with the highest value at E4 of around 1000 W/m2 at Cape Finisterre and decreasing to the South (PT1–5) and to the East (E1–3 and E5). For the Spain Mediterranean set of locations (E6–9) we also find agreement with Kalogeri et al. (2017), with the highest mean wind energy in the Gulf of Lions (E6), around 1500 W/m2 and much lower values in the other locations.

The mean wave power also shows similar behavior (Fig. 4b). The highest values are for the Irish coast with values between 60 and 70 kW/m, a range in line with the mean value for 2001–2010 of 75–85 kW/m of Kalogeri et al. (2017), but lower than the winter average of 100 kW/m of Gallagher et al. (2014). The Portuguese coast locations show much lower mean wave power, in the 20–30 kW/m range, decreasing towards the South, in agreement with the estimates of Mota and Pinto (2014). The same range is found for the Atlantic Spain locations, in agreement with the findings of Iglesias and Carballo (2010). The Spanish Mediterranean locations show the lowest wave energy potential, in line with Kalogeri et al. (2017).

Table 2
Length of observational datasets at the assessment locations of Fig. 1. Dates of first and last observations were determined from all locations in each region. The average number of observations is the average of the number of valid altimeter observations for each location in each zone.

Assessment locations	Date of 1st observation	Date of last observation	Average number of observations
Ireland (IE1–4)	02/08/91	27/12/18	5015
Portugal (PT1–5)	03/08/91	22/12/18	4647
Spain Atl. (E1–5)	19/02/91	29/12/18	2916
Spain Med. (E6–9)IE4	02/08/91	25/12/18	36,808

3.3. Wave and wind power correlation

The results for $\tau(P_a, P_w)$ show that the wind and wave power correlations are higher for the Mediterranean locations and Ireland than for Portugal and Atlantic Spain (Fig. 5).

We note that the zero-lag correlations were computed using the complete time series. Monthly or seasonal average correlation coefficients can be lower (see e.g., (Fusco et al., 2010) for the Irish coasts). In Ireland, there isn't a significant change in $\tau(P_a,P_w)$ as we move along the coast (Fig. 1a). The locations on the Portuguese coast have $\tau(P_a,P_w)$ in the vicinity of 0.5, decreasing towards the south. The Spanish Atlantic locations generally tend to decrease from the northwest corner to the Bay of Biscay.

The Mediterranean locations have the highest correlation. The general trend is a decrease from the northern location in the Gulf of Lions (E6; Fig. 1b) which has a correlation coefficient above 0.8, to the southernmost location (E9; Fig. 1b), in the Western Mediterranean Basin with $\tau(P_a,P_w)$ slightly below 0.8. The high correlation values are caused by the absence of significant swells in the area, which has its wave climate dominated by local seas. This is especially true in the Gulf of Lions, where the highest correlation was obtained.

3.3. Coefficients of variation

Given the random nature of waves and their variability, we cannot ignore that wave power is also modified by wave variability (Reguero et al., 2015). Due to temporal variations, those sites characterized by high amounts of wave energy are not always the ideal locations for wave energy collecting (Besio et al., 2016). Knowledge of the variability matters for the design of devices and can reduce or enhance the efficiency of the WECs.

To get a comprehensive analysis of the wave power assessment, we estimated the typical coefficients of variability described in Section 2.4. The COV shows a negative correlation with the mean wave power. The locations with the highest COV are those of the Mediterranean (Spain), while those with the highest wave power have lower COV (Fig. 6).

The COV of the mean wind power varies between 1 and 2 (Fig. 6a). The Irish locations and the Portuguese locations appear as clusters, while the Spanish locations exhibit a widespread COV value. The lowest COV occurs on the west coast of Ireland, in the northwestern corner of the Iberian Peninsula (E4) and in the Gulf of Lions (E6). These zones have the highest mean wind power (Fig. 6a and (Kalogeri et al., 2017)). The remaining Spanish locations are in regions with low mean wind power and where topographic effects are significant and therefore, exhibit the highest COV of the study set.

In the COV of the mean wave power (Fig. 6b), four clusters can be identified: the Mediterranean cluster (E7–9) with the highest COV and lowest mean wave power; the northern Iberian cluster (E2,E3 and E5), with the second highest mean wave power; the western Iberian cluster (PT1–5, E1, and E4) that has the lowest COV and the western Irish cluster (IRE1–4) with the highest mean wave power and low COV.

The SVI (expression 6, Section 2.4) of the mean wind power (Fig. 7a) shows a similar distribution to the COV (Fig. 6a). For the SVI of the mean wave power (Fig. 7b), the distribution is similar with respect to the Irish and West Mediterranean locations. The Iberian locations, on the other hand, are spread over the SVI range, although the Portuguese locations appear mostly in the upper range, while the Spanish locations appear predominantly in the lower part of the SVI range.

4. Discussion

The use of altimeters can provide site estimates of wind and wave power, provided wave periods can be estimated from the altimeter data. since the seminal work of Davies et al. (1997), several methods to

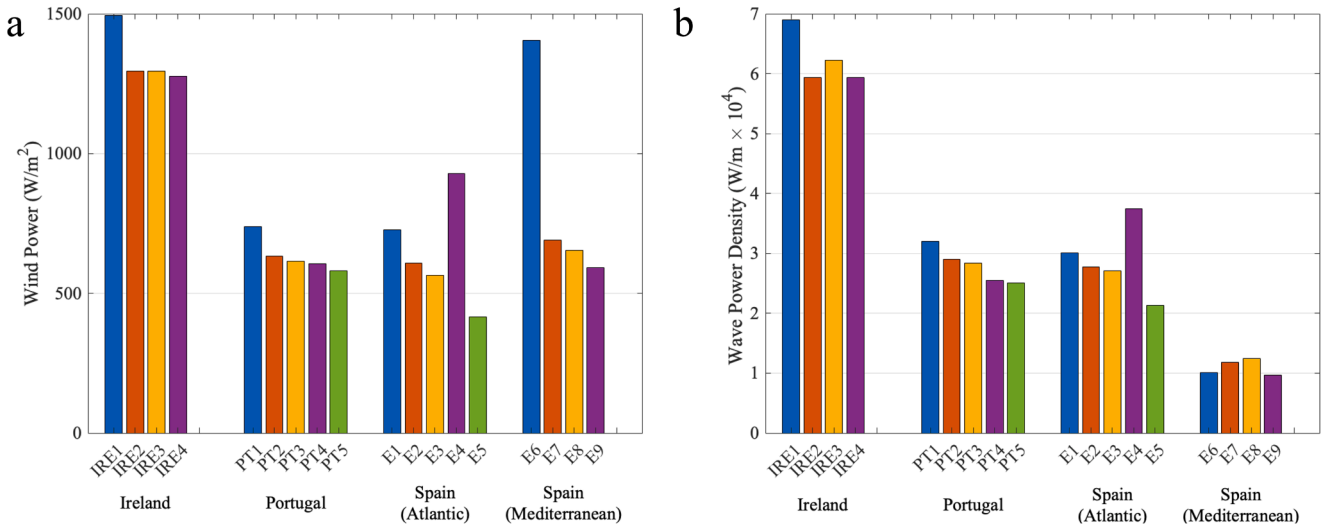

Fig. 4. Mean wind and wave power. a) Mean wind power. b) Mean wave power.

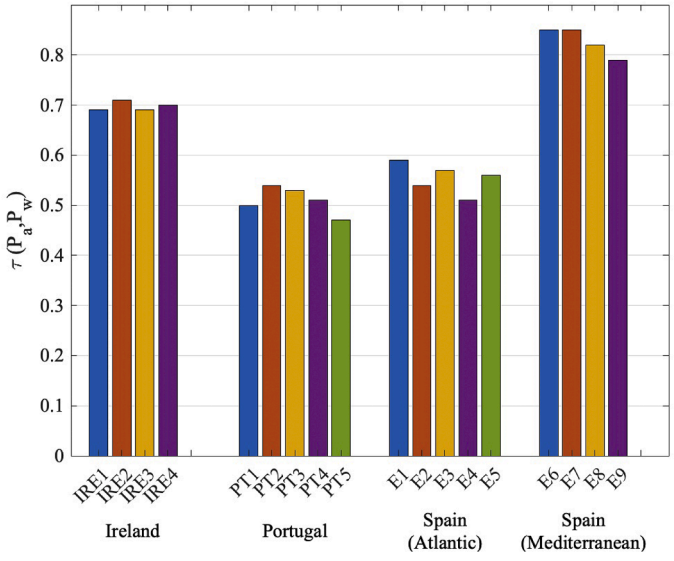

Fig. 5. Zero-lag correlation coefficient $\tau(P_a,P_w)$ between wave and wind power.

estimate the wave period from altimeter observations were developed, from the fetch-dependent semi-empirical formulas of Hwang et al. (1998) to the neural network approach of Quilfen et al. (2004). The method used in this paper used an empirical relationship between the wave period and the altimeter significant wave height (Hs) and radar cross-section σ^0. The empirical method of Gommenginger et al. (2003) can provide the wave period estimates that are needed to compute the wave power density. Although the errors introduced by the empirical method, which only used the Ku-band Hs and σ^0, are acceptable, the combination of Ku and C-band measurements can improve the wave period estimates (Zhao et al., 2012).

Another issue with the semi-empirical wave period models is related to the validity of the relationships between wind speed (or σ^0) and wave period for fully developed seas. Kshatriya et al. (2005) proposed an algorithm for altimeter wave period based on the pseudo wave age ξ, to distinguish wind-sea from swell sea states, using TOPEX data in the Arabian Sea and the Gulf of Bengal, while Mackay et al. (2008) used a multi-mission database to develop a two-piece algorithm for the altimeter derived wave period, based on a threshold value of σ^0, above which σ^0 appears not to be related to the wave period. Zhao et al. (2012) compared the results of several altimeter estimates of wave period with a new method that also used the pseudo wave age and found comparable root mean square errors of ~1 s and biases that varied from −0.35 s to

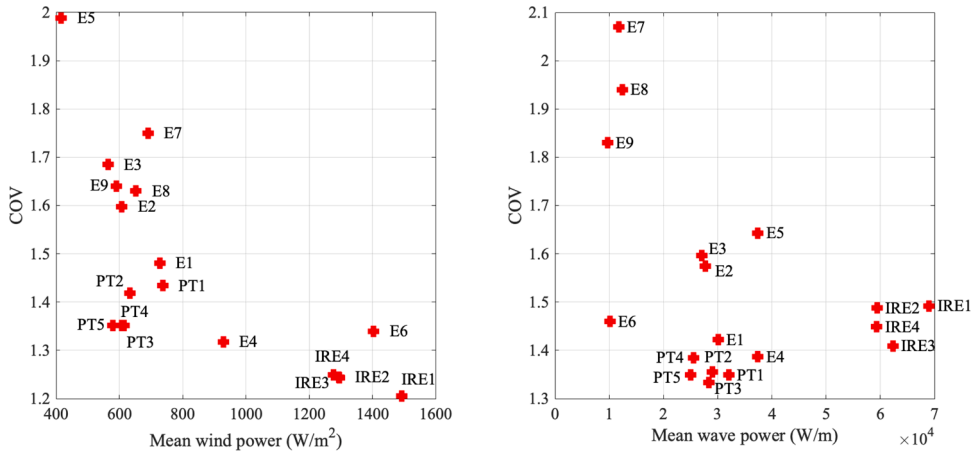

Fig. 6. Coefficient of variation at the study locations of Fig. 1. Left panel: Mean wind power; Right panel: Mean wave power; Locations: IRE1–4: West coast of Ireland (Atlantic); PT1–5: West coast of mainland Portugal (Atlantic); E1–3 and E5: North coast of Spain (Atlantic); E4: West coast of Spain (Atlantic); E6–9: West coast of Spain (Mediterranean).

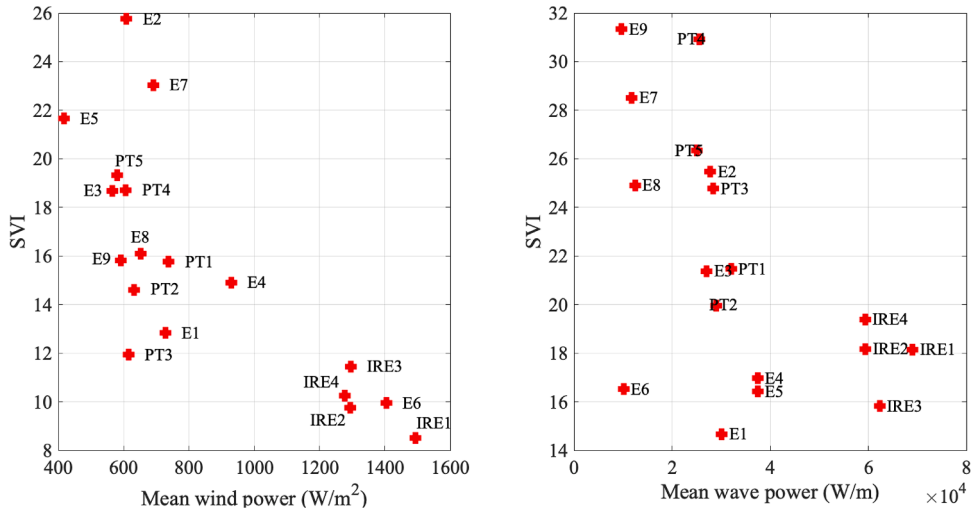

Fig. 7. Seasonal variability indicator at the study locations of Fig. 1. Left panel: Mean wind power; Right panel: Mean wave power. For the zones, see the caption of Fig. 4.

0.01 s. As such, the results obtained in this study with the Gommenginger et al. (2003) method are within the expected range. So whether or not the wave age is an issue in wave period estimates from satellite altimeters still remains an open question, which deserves further study.

The distribution of wave and wind power are consistent with other studies such as Kalogeri et al. (2017), which also found that the wave power density was larger on the Irish west coast and around the northwestern Iberian peninsula. The wave power level is somewhat constant over the entire west coast of Ireland, likely due to the large-scale swell fields that hit that region, especially in winter (Gallagher et al., 2014). When compared to the other sites, both COV and SVI are smaller for the Irish area, which favours the west coast of Ireland for renewable energy projects from a point of view of reduced variability of energy supply (Ringwood and Brandle, 2015). A similar relationship between exposure to swells and COV was found by (Zheng et al., 2013) for the China Seas.

On the other hand, the sites on the Atlantic façade of the Iberian Peninsula have a lower correlation between the wind and wave renewable energy resources than the Mediterranean-facing coasts, so they are more attractive from the point view of combined exploitation of these resources, including reduced variability of the combined power supply (Fusco et al., 2010; Kalogeri et al., 2017).

5. Conclusions

Using North Atlantic and Mediterranean European sites as comparators for wind/wave correlation, we show that wind/wave energy is relatively correlated in the Mediterranean sites but not in the Western North Atlantic sites, which has implications for the efficient combination of renewable energy sources to increase the resiliency of the renewable energy supply. Our contention is that the increased correlation in the Mediterranean areas is due to the fact that wind and wave resources are ultimately generated by local wind, while the North Atlantic swell is not correlated with local coastal wind.

The collocation of wind and wave farms (hybrid farms) only has a strong rationale in locations where the wind and wave energy resources are relatively uncorrelated. Thus, the European coasts facing the Atlantic Ocean are clearly the most adequate place for this purpose.

The different characteristics of the studied sites show some correspondence between variability and mean wave power which is an essential input to a marine renewable energy strategy in any jurisdiction. The level of variability decreases with an increase in mean wave power, undoubtedly since the higher power waves are caused by swell, while wind waves have higher variability.

Satellite altimetry was used to estimate wind and wave power resources in the European coastal waters at the study locations. The ESA SS_cci database provided a 27-year time series of sea state variables, and the Gommenginger et al. (2003) method was used to estimate the wave period. The wave/wind power assessment presented here will be extended to other coastal locations worldwide.

Funding

This research was funded by the European Space Agency Visiting Scientist program, where the first author was enrolled in 2022.

CRediT authorship contribution statement

Sonia Ponce de León: Writing – review & editing, Writing – original draft, Validation, Methodology, Investigation, Formal analysis, Conceptualization. **João Horta Bettencourt:** Writing – review & editing, Methodology, Investigation, Formal analysis, Conceptualization. **John V. Ringwood:** Writing – review & editing, Conceptualization. **Jérôme Benveniste:** Writing – review & editing, Resources, Funding acquisition.

Declaration of competing interest

The authors declare that they have no known competing financial interests or personal relationships that could have appeared to influence the work reported in this paper.

Data availability

https://climate.esa.int/en/projects/sea-state/data/

Acknowledgements

The first author heartedly acknowledges Dr Jérôme Benveniste, who encouraged her to apply for a Visiting Scientist stay at ESA. She also acknowledges the European Space Agency for the support provided. JHB acknowledges postdoctoral support from the European Union's Horizon 2020 research and innovation program under the Marie Skłodowska-Curie grant agreement No 101034309. This work also contributes to the Strategic Research Plan of the centre for Marine Technology and Ocean Engineering (CENTEC), which is financed by the Portuguese Foundation for Science and Technology (Fundação para a Ciência e Tecnologia -

FCT) under UIDB/UIDP/00134/2020.

References

Abdalla, S., et al., 2021. Altimetry for the future: building on 25 years of progress. Adv. Space Res. 68, 319–363. https://doi.org/10.1016/j.asr.2021.01.022, 25 Years of Progress in Radar Altimetry.

Ambühl, S., Kofoed, J.P., Sørensen, J.D., 2014. Stochastic modeling of long-term and extreme value estimation of wind and sea conditions for probabilistic reliability assessments of wave energy devices. Ocean Eng 89, 243–255. https://doi.org/10.1016/J.OCEANENG.2014.08.010.

Astariz, S., Iglesias, G., 2017. The collocation feasibility index – A method for selecting sites for co-located wave and wind farms. Renew. Energy 103, 811–824. https://doi.org/10.1016/j.renene.2016.11.014.

Astariz, S., Iglesias, G., 2016. Selecting optimum locations for co-located wave and wind energy farms. Part II: a case study. Energy Convers. Manag. 122, 599–608. https://doi.org/10.1016/j.enconman.2016.05.078.

Besio, G., Mentaschi, L., Mazzino, A., 2016. Wave energy resource assessment in the Mediterranean Sea on the basis of a 35-year hindcast. Energy 94, 50–63. https://doi.org/10.1016/j.energy.2015.10.044.

Brown, A.G., Neill, S., Lewis, M., 2013. The influence of wind gustiness on estimating the wave power resource. Int. J. Mar. Energy 3, e1–e9. https://doi.org/10.1016/J.IJOME.2013.11.007.

Cahill, B., Lewis, T., 2014. Wave periods and the calculation of wave power.

Carvalho, D., Rocha, A., Gómez-Gesteira, M., Silva Santos, C., 2017. Offshore winds and wind energy production estimates derived from ASCAT, OSCAT, numerical weather prediction models and buoys – A comparative study for the Iberian Peninsula Atlantic coast. Renew. Energy 102, 433–444. https://doi.org/10.1016/j.renene.2016.10.063.

Carvalho, D., Rocha, A., Gómez-Gesteira, M., Silva Santos, C., 2014. Offshore wind energy resource simulation forced by different reanalyses: comparison with observed data in the Iberian Peninsula. Appl. Energy 134, 57–64. https://doi.org/10.1016/j.apenergy.2014.08.018.

Chen, Y., Yu, X., 2017. Sensitivity of storm wave modeling to wind stress evaluation methods. J. Adv. Model. Earth Syst. 9, 893–907. https://doi.org/10.1002/2016MS000850.

Davies, C..G., Challenor, P.G., Cotton, P.D., 1997. Measurement of wave period from radar altimeters. In: Edge, B.L., Hemsley, J.M. (Eds.). American society of civil engineers, USA, pp. 819–826.

deCastro, M., Costoya, X., Salvador, S., Carvalho, D., Gómez-Gesteira, M., Sanz-Larruga, F.J., Gimeno, L., 2019. An overview of offshore wind energy resources in Europe under present and future climate. Ann. N. Y. Acad. Sci. 1436, 70–97. https://doi.org/10.1111/nyas.13924.

Dodet, G., Piolle, J.F., Quilfen, Y., Abdalla, S., Accensi, M., Ardhuin, F., Ash, E., Bidlot, J. R., Gommenginger, C., Marechal, G., Passaro, M., Quartly, G., Stopa, J., Timmermans, B., Young, I., Cipollini, P., Donlon, C., 2020. The Sea State CCI dataset v1: towards a sea state climate data record based on satellite observations. Earth Syst. Sci. Data 12, 1929–1951. https://doi.org/10.5194/essd-12-1929-2020.

Fusco, F., Nolan, G., Ringwood, J.V., 2010. Variability reduction through optimal combination of wind/wave resources – An Irish case study. Energy 35, 314–325. https://doi.org/10.1016/j.energy.2009.09.023.

Gallagher, S., Tiron, R., Dias, F., 2014. A long-term nearshore wave hindcast for Ireland: atlantic and Irish Sea coasts (1979–2012). Ocean. Dyn. 64, 1163–1180. https://doi.org/10.1007/s10236-014-0728-3.

Globwave Team, 2013. GlobWave final report (Tech. report no. deliverable D.30).

Goddijn-Murphy, L., Martín Míguez, B., McIlvenny, J., Gleizon, P., 2015. Wave energy resource assessment with AltiKa satellite altimetry: a case study at a wave energy site. Geophys. Res. Lett. 42, 5452–5459. https://doi.org/10.1002/2015GL064490.

Gommenginger, C.P., Srokosz, M.A., Challenor, P.G., Cotton, P.D., 2003. Measuring ocean wave period with satellite altimeters: a simple empirical model. Geophys. Res. Lett. 30 https://doi.org/10.1029/2003GL017743.

Guillou, N., Lavidas, G., Chapalain, G., 2020. Wave energy resource assessment for exploitation—a review. J. Mar. Sci. Eng. 8, 705. https://doi.org/10.3390/jmse8090705.

Huang, N.E., Shen, Z., Long, S.R., Wu, M.C., Shih, H.H., Zheng, Q., Yen, N.C., Tung, C.C., Liu, H.H., 1998. The empirical mode decomposition and the Hilbert spectrum for nonlinear and non-stationary time series analysis. Proc. R. Soc. Lond. Ser. Math. Phys. Eng. Sci. 454, 903–995. https://doi.org/10.1098/rspa.1998.0193.

Hwang, P.A., Teague, W.J., Jacobs, G.A., Wang, D.W., 1998. A statistical comparison of wind speed, wave height, and wave period derived from satellite altimeters and ocean buoys in the Gulf of Mexico region. J. Geophys. Res. Oceans 103, 10451–10468. https://doi.org/10.1029/98JC00197.

Iglesias, G., Carballo, R., 2010. Offshore and inshore wave energy assessment. Asturias (N Spain). Energy 35, 1964–1972. https://doi.org/10.1016/j.energy.2010.01.011.

Kalogeri, C., Galanis, G., Spyrou, C., Diamantis, D., Baladima, F., Koukoula, M., Kallos, G., 2017. Assessing the European offshore wind and wave energy resource for combined exploitation. Renew. Energy 101, 244–264. https://doi.org/10.1016/j.renene.2016.08.010.

Kshatriya, J., Sarkar, A., Kumar, R., 2005. Determination of ocean wave period from altimeter data using wave-age concept. Mar. Geod. 28, 71–79. https://doi.org/10.1080/01490410590884575.

Mackay, E.B.L., Retzler, C.H., Challenor, P.G., Gommenginger, C.P., 2008. A parametric model for ocean wave period from Ku band altimeter data. J. Geophys. Res. Oceans 113.

Martini, M., Guanche, R., Losada-Campa, I., Losada, I.J., 2018. The impact of downtime over the long-term energy yield of a floating wind farm. Renew. Energy 117, 1–11. https://doi.org/10.1016/j.renene.2017.10.032.

Mota, P., Pinto, J.P., 2014. Wave energy potential along the western Portuguese coast. Renew. Energy 71, 8–17. https://doi.org/10.1016/j.renene.2014.02.039.

Piollé, J.F., Dodet, G., Quilfen, Y., 2020. ESA sea state climate change initiative (Sea_State_cci): global remote sensing multi-mission along-track significant wave height, L2P product, version 1.1. https://doi.org/10.5285/F91CD3EE7B6243D5B7D41B9BEAF397E1.

Ponce de León, S., Orfila, A., Simarro, G., 2016. Wave energy in the Balearic Sea. Evolution from a 29 year spectral wave hindcast. Renew. Energy 85, 1192–1200. https://doi.org/10.1016/j.renene.2015.07.076.

Ponce de León, S., Bettencourt, J., 2021. Composite analysis of North Atlantic extra-tropical cyclone waves from satellite altimetry observations. Adv. Space Res. https://doi.org/10.1016/j.asr.2019.07.021.

Ponce de León, S., Restano, M., Benveniste, J, 2023. Assessment of wave power density using sea state climate change initiative database in the French façade. J. Mar. Sci. Eng. 11, 1970. https://doi.org/10.3390/jmse11101970.

Ponce de León, S., Restano, M., Benveniste, J., 2024. Assessing the wave power density in the atlantic french façade from high-resolution CryoSat-2 SAR altimetry data. Energy. ISSN: 0360-5442 302, 131712. https://doi.org/10.1016/j.energy.2024.131712.

Pontes, M.T., 1998. Assessing the European wave energy resource. J. Offshore Mech. Arct. Eng. 120, 226–231. https://doi.org/10.1115/1.2829544.

Probst, O., Cárdenas, D., 2010. State of the art and trends in wind resource assessment. Energies. 3, 1087–1135. https://doi.org/10.3390/EN3061087.

Quilfen, Y., Chapron, B., 2021. On denoising satellite altimeter measurements for high-resolution geophysical signal analysis. Adv. Space Res. 68, 875–891. https://doi.org/10.1016/j.asr.2020.01.005, 25 Years of Progress in Radar Altimetry.

Quilfen, Y., Chapron, B., Collard, F., Serre, M., 2004. Calibration/validation of an altimeter wave period model and application to TOPEX/Poseidon and Jason-1 altimeters. Mar. Geod. 27, 535–549.

Reguero, B.G., Losada, I.J., Méndez, F.J., 2015. A global wave power resource and its seasonal, interannual and long-term variability. Appl. Energy 148, 366–380. https://doi.org/10.1016/j.apenergy.2015.03.114.

Ringwood, J.V., Brandle, G., 2015. A new world map for wave power with a focus on variability. In: Proceedings of 11th European wave and tidal energy conference. presented at the 11th EWTEC. Nantes, France.

Soukissian, T., Karathanasi, F., Axaopoulos, P., 2017. Satellite-based offshore wind resource assessment in the mediterranean sea. IEEE J. Ocean. Eng. 42, 73–86. https://doi.org/10.1109/JOE.2016.2565018.

Stoutenburg, E.D., Jacobson, M.Z., 2010. Optimizing offshore transmission links for marine renewable energy farms. OCEANS 2010 MTS/IEEE seattle. presented at the oceans 2010 MTS/IEEE Seattle, pp. 1–9. https://doi.org/10.1109/OCEANS.2010.5664506.

Stoutenburg, E.D., Jenkins, N., Jacobson, M.Z., 2010. Power output variations of co-located offshore wind turbines and wave energy converters in California. Renew. Energy 35, 2781–2791. https://doi.org/10.1016/j.renene.2010.04.033.

Yaakob, O., Hashim, F.E., Mohd Omar, K., Md Din, A.H., Koh, K.K., 2016. Satellite-based wave data and wave energy resource assessment for South China Sea. Renew. Energy 88, 359–371. https://doi.org/10.1016/j.renene.2015.11.039.

Wan, Y., Zhang, J., Meng, J., Wang, J., Dai, Y., 2016. Study on wave energy resource assessing method based on altimeter data—A case study in Northwest Pacific. Acta Oceanol. Sin. 35, 117–129. https://doi.org/10.1007/s13131-016-0804-2.

Zhao, D., Li, S., Song, C., 2012. The comparison of altimeter retrieval algorithms of the wind speed and the wave period. Acta Oceanol. Sin. 31, 1–9.

Zheng, C., 2021. Global oceanic wave energy resource dataset—With the Maritime Silk Road as a case study. Renew. Energy 169, 843–854. https://doi.org/10.1016/j.renene.2021.01.058.

Zheng, C., Pan, J., Li, J., 2013. Assessing the China Sea wind energy and wave energy resources from 1988 to 2009. Ocean Eng 65, 39–48. https://doi.org/10.1016/j.oceaneng.2013.03.006.